Equivalent Static Wind Loads on Buildings: New Model

Xinzhong Chen[1] and Ahsan Kareem[2]

Abstract: In current design practice, spatiotemporally varying wind loads on buildings are modeled as equivalent static wind loads. This loading description serves as pivotal information for estimating response under the combined action of wind and other loads. This paper presents a framework for evaluating the equivalent static wind load for any given peak response of buildings with uncoupled responses in the three primary directions. A new description of the background loading based on the gust loading envelope/peak dynamic loading is presented. The resonant loading is expressed in terms of the inertial load following the respective fundamental structural mode. The equivalent static wind loading for the total peak response is then expressed as a linear combination of the background and resonant components. Following this framework, closed-form formulations using an analytical wind loading model are presented. The gust response factors and the equivalent static wind loads for various alongwind response components at different building elevations are discussed in detail highlighting the advantages of the proposed equivalent static loading. The potential high-frequency force balance technique for ascertaining the equivalent static loading on buildings is also revisited. A commentary is presented to highlight the role of mode shape correction, uncertainty in the modeling of wind loads, and contributions of higher modes to background response.

Introduction

In current design practice, spatiotemporally varying wind loads on buildings are modeled as equivalent static wind loads (ESWLs). This loading description serves as pivotal information for estimating the response under the combined action of wind and other loads, through a simple static analysis procedure, to ensure structural safety and serviceability. The traditional gust response factor (GRF) approach (Davenport 1967) is widely used in most current building design codes and standards for the along-wind response that results in a load distribution similar to the mean wind load (e.g., Zhou and Kareem 2001). Similar GRF concepts have been adopted for the acrosswind and torsional response components (Piccardo and Solari 2000; Kareem and Zhou 2003). The GRF approach is simple to use in the building design process, however, the GRFs may vary over a wide range for different response components of a structure and may have significantly different values for structures with similar geometric profile and associated wind load characteristics but different structural systems. For the acrosswind and torsional responses, which are typically characterized by low values of mean wind loading and associated response, particularly, in the cases of symmetric buildings, the corresponding GRFs may not have the same

[1] Assistant Professor, Dept. of Civil Engineering, Texas Tech Univ., Lubbock TX 79409

[2] Professor, Dept. of Civil Engineering and Geological Sciences, Univ. of Notre Dame, Notre Dame, IN 46556. E-mail: kareem@nd.edu

physical meaning as the traditional GRF for the alongwind response.

Similar to the GRF approach, an ESWL description based on the peak dynamic pressure/wind load (including the mean load) has been adopted in some building design codes, such as the draft Eurocode (ENV-1991) (CEN 1994), ASCE7-02, and the new Australian/New Zealand Standards (Holmes 2002a). This format describes the ESWL as the peak dynamic load multiplied by a constant coefficient referred to as dynamic response factor (DRF) (Holmes 2002a). The DRF was defined as the ratio of the peak dynamic response (including the mean, background, and resonant components) to the response caused by the peak dynamic load that includes the mean and the background load effects but excludes the reduction effects due to the loss of correlation in wind loading. In Repetto and Solari (2004), an identical ESWL distribution for all response components was suggested utilizing a polynomial expansion determined on the premise that the ESWL results in accurate estimates of a limited number of preselected peak responses.

Taking advantage of the spectral descriptions of wind loads and their effects on buildings, separation of the dynamic response (excluding the mean component) and the associated ESWL into background (quasi-static) and resonant components provides a more efficient response prediction framework and a physically more meaningful description of loading [Davenport 1985; Kasperski 1992; Holmes and Kasperski 1996; Holmes 2002b; Isyumov 1999; Zhou et al. 2000; Zhou and Kareem 2001; Chen and Kareem 2000; 2001, Kareem and Chen 2004; Piccardo and Solari 2002]. The resonant ESWL (RESWL) can be expressed in terms of the inertial load in each structural mode, which depends on the mass distribution and mode shape (e.g., Davenport 1985). The background ESWL (BESWL) depends on the external wind load characteristics. Kasperski (1992) proposed a load-response-correlation (LRC) approach for determining BESWL that results in different spatial load distributions for different response components. The LRC approach provides a most probable load distri-

bution for a desired peak response component, which has been experimentally confirmed by Tamura et al. (2002). When the background response is less important in comparison with the resonant component, which is the case in a flexible building, approximate description of the BESWL may be utilized. In Boggs and Peterka (1989) and Zhou and Kareem (2001), the BESWL for any building response was approximated by the mean wind load distribution multiplied by the gust response factor for the background base bending moment. In this case, as the background response is often approximated by the respective fundamental mode response, the BESWL can also be given in terms of the modal inertial load similar to the RESWL (Chen and Kareem 2001).

Once the RESWL in each structural mode and the BESWL have been determined, the corresponding peak resonant and background responses are calculated using a static analysis. These are then combined using the complete quadratic combination (CQC) approach or the square root of the sum of squares (SRSS) approach for the total peak response (excluding the mean component). Alternatively, an ESWL for the total peak response can be expressed as a linear combination of the background and resonant loading components. An approach for combining the background and uncoupled multimodal inertial loads was presented in Holmes (2002b). Chen and Kareem (2001) proposed an analysis framework that combines the background and coupled multimodal inertial loads. This scheme has been applied to long-span bridges with multimode coupled buffeting responses, and can also be utilized for tall buildings with three-dimensional (3D) mode shapes and closely spaced fundamental mode frequencies (Kareem and Chen 2004). It is important to note that the ESWL for the total peak response cannot be determined by combining the background and resonant loading components using CQC or SRSS approaches, although a similar scheme has been suggested in literature (e.g., Holmes and Kasperski 1996). Alternatively, when both the background and resonant response are approximated by the fundamental mode response, the ESWL for the total peak response can be described in terms of inertial load involving both background and resonant components.

In this paper, an analysis framework is presented for evaluating the ESWL for any given peak response component of wind-excited buildings with uncoupled responses in the three primary directions. A new description of the BESWL is presented based on the gust loading envelope (peak dynamic loading without the mean component). The RESWL is given in terms of the inertial load in each fundamental mode. The ESWL for the total peak response is then expressed as a linear combination of the BESWL and RESWL. Based on this framework, closed-form formulations using an analytical wind loading model are presented. The gust response factors and the ESWLs for various alongwind response components at different building elevations are discussed in detail highlighting the advantages of the proposed ESWL description. The high-frequency force balance (HFFB) technique is also revisited in the context of determining the equivalent static loading on buildings. Finally, a commentary is provided regarding mode shape correction and uncertainty in the modeling of wind loads as well as contributions of higher modes to background response.

General Formulations

A wind-excited building with one-dimensional uncoupled mode shapes in two orthogonal translational and rotational directions at a given wind speed and direction is considered (Fig. 1). The wind
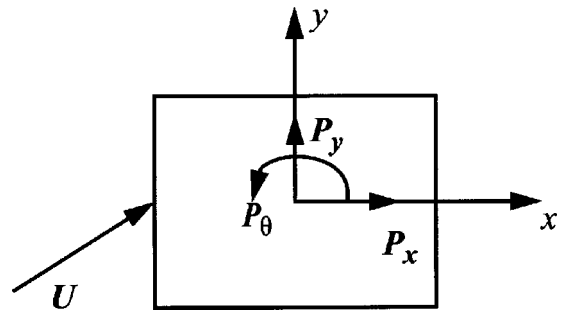

Fig. 1. Coordinate system and wind orientation

loads per unit height at elevation z above the ground have mean components of $\bar{P}_x(z)$, $\bar{P}_y(z)$, and $\bar{P}_\theta(z)$, and fluctuating components of $P_x(z,t)$, $P_y(z,t)$, and $P_\theta(z,t)$, in two translational axes x and y and about the vertical axis z. Discussion here is focused on the response with one-dimensional influence functions in the three primary directions. The uncoupled class of response in the three primary directions permits discussion of wind loading and building response in each direction independently. Without loss of generality, the following discussion will focus on translational response in the x direction at a given wind speed and orientation; formulations in other directions are immediate.

For a specific response of interest (displacement, bending moment, shear force, and member forces) at a building elevation z_0, $R(z_0,t)$, the mean (static) and background components can be calculated by the static and quasi-static analysis. The resonant component can be analyzed using modal analysis involving only the fundamental mode. The mean response and root mean square (RMS) background and resonant responses are expressed as

$$\bar{R} = \int_0^H \bar{P}_x(z)\mu_x(z)dz \tag{1}$$

$$\sigma_{R_b} = \sqrt{\int_0^H \int_0^H \mu_x(z_1)\mu_x(z_2)R_{P_{xx}}(z_1,z_2)dz_1dz_2} \tag{2}$$

$$\sigma_{R_r} = \frac{\int_0^H m(z)\Theta_x(z)\mu_x(z)dz}{\int_0^H m(z)\Theta_x^2(z)dz}\sqrt{\frac{\pi}{4\xi_1}f_1 S_{Q_x}(f_1)} \tag{3}$$

$$S_{Q_x}(f) = \int_0^H \int_0^H \Theta_x(z_1)\Theta_x(z_2)S_{P_{xx}}(z_1,z_2,f)dz_1dz_2 \tag{4}$$

where H=building height; $\mu_x(z)$=influence function indicating the response $R(z_0,t)$ under unit load acting at the height z in x direction; $\Theta_x(z)$=fundamental mode shape; f_1 and ξ_1=fundamental frequency and damping ratio (including aerodynamic damping), respectively; $m(z)$=mass per unit height; $R_{P_{xx}}(z_1,z_2)$ and $S_{P_{xx}}(z_1,z_2,f)$=covariance and cross power spectral density (XPSD) between $P_x(z_1,t)$ and $P_x(z_2,t)$; $S_{Q_x}(f)$=power spectral density (PSD) of the generalized modal force.

It is noted that background response analysis using influence functions implicitly includes the contributions of all structural

modes, thus it provides a more accurate estimate of response in comparison with modal analysis involving only the fundamental mode.

Peak dynamic response (excluding the mean response), R_{max}, is obtained by combining the background and resonant components:

$$R_{max} = \sqrt{g_b^2 \sigma_{R_b}^2 + g_r^2 \sigma_{R_r}^2} \tag{5}$$

where g_b and g_r=peak factors for the background and resonant responses, respectively, typically ranging in value between 3 and 4.

Following the LRC approach, the BESWL for peak background response, $R_{b\,max}=g_b \sigma_{R_b}$, is given by:

$$F_{eR_b}(z) = \frac{g_b}{\sigma_{R_b}} \int_0^H \mu_x(z_1) R_{P_{xx}}(z,z_1) dz_1 \tag{6}$$

which depends on the influence function of the response under consideration and thus the BESWL has a different spatial distribution for different response components. The LRC approach results in a most probable load distribution for a given peak background response. However, since in this approach each response component corresponds to a different spatial load distribution, this feature may limit its potential application to design standards or practice. An approximate modeling of the BESWL based on the LRC approach has been presented in Holmes (1996) by eliminating the influence of the influence function of the response.

For the purpose of a pragmatic modeling of the BESWL, it is proposed here to express the BESWL as the gust loading envelope (GLE), $F'_{ebx}(z)$, multiplied by a background factor, B_z,

$$F_{eR_b}(z) = B_z F'_{ebx}(z) = B_z g_b \sqrt{R_{P_x}(z)} \tag{7}$$

$$B_z = \sigma_{R_b}/\sigma'_{R_b}; \qquad \sigma'_{R_b} = \int_0^H \mu_x(z) F'_{ebx}(z) dz/g_b \tag{8}$$

where $R_{P_x}(z) = R_{P_{xx}}(z,z)$; $g_b \sigma'_{R_b}$=peak background response under the loading envelope that does not include the effect due to loss of spatial correlation in wind load over the building height; B_z represents the reduction effect with respect to the response $R(z_0,t)$ due to loss of correlation of wind loading. In cases where the wind loads are fully correlated, i.e., $R_{P_{xx}}(z_1,z_2) = \sqrt{R_{P_x}(z_1)R_{P_x}(z_2)}$, B_z reduces to unity and the BESWLs based on the LRC and GLE approaches converge to the gust loading envelope, $F'_{ebx}(z)$.

The RESWL for the peak resonant response, $R_{r\,max}=g_r \sigma_{R_r}$, is given in terms of the inertial load distribution:

$$F_{erx}(z) = \frac{g_r m(z) \Theta_x(z)}{\int_0^H m(z) \Theta_x^2(z) dz} \sqrt{\frac{\pi}{4\xi_1} f_1 S_{Q_x}(f_1)} \tag{9}$$

which can also be expressed in terms of distributing the peak base bending moment or base shear force over the building height following the inertial load distribution. When torsional response is under consideration, the RESWL is obtained by distributing the base torque over the building height.

The ESWL for the total peak dynamic response, R_{max}, can be provided as a linear combination of the background and resonant loads (Boggs and Peterka 1989; Chen and Kareem 2000, 2001; Holmes 2002b):

$$F_{eR}(z) = [g_b \sigma_{R_b} B_z F'_{ebx}(z) + g_r \sigma_{R_r} F_{erx}(z)]/\sqrt{g_b^2 \sigma_{R_b}^2 + g_r^2 \sigma_{R_r}^2} \tag{10}$$

It is obvious from Eq. (10) that any peak response can be expressed as a linear combination of the static response under the gust loading envelope, $F'_{ebx}(z)$, and the modal inertial load, $F_{erx}(z)$. The combination/weighting factors vary for the response component under consideration, which may be simplified through a parametric study for a range of response components for potential application to building codes and standards. For the peak response including the mean component, the ESWL should be given as $\bar{P}_x(z) \pm F_{eR}(z)$.

Closed-Form Formulation

In the following, closed-form formulations based on an assumed analytical loading model are presented for the response in the translational direction, x, which can be extended conveniently to the response components in the other two directions.

The mass per unit height, $m(z)$, the first mode shape, $\Theta_x(z)$, and the influence function of the response $R(z_0,t)$, $\mu_x(z)$, are expressed as

$$m(z) = m_0 \left(1 - \lambda \frac{z}{H}\right); \quad \Theta_x(z) = \left(\frac{z}{H}\right)^\beta \tag{11}$$

$$\mu_x(z) = \begin{cases} \mu_0 \left(\dfrac{z-z_0}{H}\right)^{\beta_0} & (z \geq z_0) \\ 0 & (z < z_0) \end{cases} \tag{12}$$

where m_0=the mass per unit height at the bottom of the building; λ=a constant parameter $(0 \leq \lambda \leq 1)$; and β=mode shape exponent ranging between 1.0 and 1.5 for typical buildings; μ_0 and β_0=constant parameters. For the top displacement, $Y_x(t)$, $\mu_0=i_0$, $z_0=0$, and $\beta_0=\beta'$ (where i_0 is the deflection at the top of the building under a unit load at that point; β'=a constant parameter); for the bending moment at elevation z_0, $M_x(z_0,t)$, $\mu_0=H$ and $\beta_0=1$; and for the shear force at elevation z_0, $F_x(z_0,t)$, $\mu_0=1$, and $\beta_0=0$.

The XPSD and covariance of wind load per unit height are assumed as

$$S_{P_{xx}}(z_1,z_2,f) = \frac{S_P(f)}{H^2} \left(\frac{z_1}{H}\right)^\alpha \left(\frac{z_2}{H}\right)^\alpha \exp\left(-\frac{k_z f}{U_H}|z_1 - z_2|\right) \tag{13}$$

$$R_{P_{xx}}(z_1,z_2) = \frac{\sigma_{P_b}^2}{H^2} \left(\frac{z_1}{H}\right)^\alpha \left(\frac{z_2}{H}\right)^\alpha \exp\left(-\frac{|z_1 - z_2|}{L_x^z}\right) \tag{14}$$

where $\sigma_{P_b}^2 = \int_0^{f'} S_P(f)df \approx \int_0^\infty S_P(f)df (f' \leq f_1)$; $S_P(f)$=PSD of wind load at the building top normalized by H^2; U_H=mean wind speed at the building top; α=wind load profile coefficient; L_x^z=integral length scale of the fluctuating wind load; and k_z=decay factor in the vertical direction. It should be noted that Eqs. (13) and (14) can be obtained by fitting the XPSD and covariance of wind loading, separately.

Accordingly, the RMS background and resonant components of $R(z_0,t)$ are given by

$$\sigma_{R_b} = \mu_0 F_b\left(\alpha, \beta_0, \frac{z_0}{H}\right) B_z\left(\alpha, \beta_0, \frac{z_0}{H}\right) \sigma_{P_b} \tag{15}$$
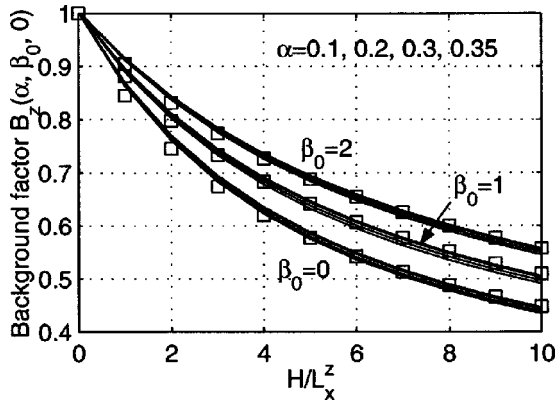
Fig. 2. Background factor $B_z(\alpha, \beta_0, 0)$

$$\sigma_{R_r} = \mu_0 F_r\left(\beta, \beta_0, \frac{z_0}{H}\right) \frac{|J_z(\alpha, \beta, f_1)|}{(1+\alpha+\beta)} \sqrt{\frac{\pi}{4\xi_1} f_1 S_P(f_1)} \qquad (16)$$

where the functions $F_b(\alpha, \beta_0, z_0/H)$, $F_r(\beta, \beta_0, z_0/H)$, $B_z(\alpha, \beta_0, z_0/H)$, and $|J_z(\alpha, \beta_0, f)|$ are defined in Appendix A.

$B_z(\alpha, \beta_0, z_0/H)$ and $|J_z(\alpha, \beta, f)|$ are the background factor and joint acceptance function, respectively, that represent the load reduction effects due to the loss of vertical spatial correlation in wind loads. As illustrated in Fig. 2 for $B_z(\alpha, \beta_0, 0)$ with $\alpha=0.1$, 0.2, 0.3 and 0.35, and $\beta_0=0$, 1, and 2 (indicated by solid lines), the background factor is insensitive to the parameter α, and can be approximated by (indicated by squares in Fig. 2)

$$B_z\left(\alpha, \beta_0, \frac{z_0}{H}\right) \approx \frac{1}{\sqrt{1+(H-z_0)/L_x^z/(2.5+\beta_0)}} \qquad (17)$$

Similarly, the joint acceptance function can be given by

$$|J_z(\alpha, \beta, f)| \approx \frac{1}{\sqrt{1+k_z f H/U_H/(2.5+\beta)}} \qquad (18)$$

The background factor in Holmes (1994) is conservatively approximated by setting the influence function parameter $\beta_0=1$:

$$B_z = \frac{1}{\sqrt{1+(H-z_0)/L_x^z/3.5}} \qquad (19)$$

It is noted that both B_z and $|J_z|$ become unity when wind loads are fully correlated over the building height, i.e., $H/L_x^z \to 0$ and $k_z f H/U_H \to 0$, and decrease with the decrease in the load correlation/coherence. For the responses induced by the localized wind load effects such as shear force and bending moment at higher elevations near the building top, i.e., z_0 is close to H, these reduction effects are less significant in comparison with the responses resulting from the integrated wind load effects acting on the entire building height such as the base shear force, base bending moment and top displacement.

The BESWL based on the GLE approach for peak response, $g_b \sigma_{R_b}$, is expressed as

$$F_{eR_b}(z) = B_z F'_{ebx}(z) = B_z \frac{g_b \sigma_{P_b}}{H}\left(\frac{z}{H}\right)^\alpha \qquad (20)$$

and the RESWL is expressed as

$$F_{erx}(z) = \frac{(2\beta+1)(2\beta+2)}{[(2\beta+2)-\lambda(2\beta+1)]} \frac{|J_z(\alpha, \beta, f)|}{(1+\alpha+\beta)} \frac{g_r}{H}$$
$$\times \sqrt{\frac{\pi}{4\xi_1} f_1 S_P(f_1)} \left(1 - \lambda \frac{z}{H}\right)\left(\frac{z}{H}\right)^\beta \qquad (21)$$

Application to the Alongwind Response

In order to highlight the advantage of the ESWL based on the external wind loading and modal inertial loads in comparison with that based on the traditional GRF approach, the following discussion is focused on the alongwind response, i.e., the response in the translational direction, x, under wind at zero angle of incidence. Utilizing strip theory, the alongwind drag force can be related to the wind fluctuations in the alongwind direction. Assuming that the mean wind speed varies according to the power law as

$$U(z) = U_H\left(\frac{z}{H}\right)^\alpha \qquad (22)$$

and assuming that the drag coefficient, aerodynamic admittance function and standard deviation turbulence are uniform over the building height, the mean wind load per unit height is given by

$$\bar{P}_x(z) = \frac{q_H}{H}\left(\frac{z}{H}\right)^{2\alpha} \qquad (23)$$

and the XPSD and covariance of wind load per unit height are given in Eqs. (13) and (14) with $L_x^z = L_u^z$ (where L_u^z is the turbulence integral length scale), and

$$S_P(f) = 4q_H^2 I_u^2 S_u^*(f)|\chi_D(f)|^2|J_y(f)|^2 \qquad (24)$$

$$\sigma_{P_b}^2 = \int_0^{f'} 4q_H^2 I_u^2 S_u^*(f)|\chi_D(f)|^2|J_y(f)|^2 df \qquad (25)$$

where $q_H=0.5\rho U_H^2 C_D BH$; $\rho=$air density; $B=$building width; C_D =drag coefficient; $S_u^*(f)=S_{u0}(f)/\sigma_{u0}^2=$normalized PSD of wind fluctuation with respect to its mean square value σ_{u0}^2 $=\int_0^\infty S_{u0}(f)df$; $I_u=\sigma_{u0}/U_H=$turbulence intensity at the top of the building; $|\chi_D(f)|^2=$aerodynamic admittance function; and $|J_y(f)|^2=$joint acceptance in the horizontal direction given by

$$|J_y(f)|^2 = \frac{1}{B^2}\int_0^B\int_0^B \exp\left(-\frac{k_y f}{U_H}|y_1-y_2|\right)dy_1 dy_2$$
$$= \frac{2}{\lambda_y}\left(1 - \frac{1}{\lambda_y} + \frac{1}{\lambda_y}e^{-\lambda_y}\right) \qquad (26)$$

and $\lambda_y=k_y fB/U_H$; and $k_y=$decay factor in horizontal direction.

Accordingly, the mean response of $R(z_0, t)$ is expressed as

$$\bar{R} = q_H\mu_0\bar{F}\left(\alpha, \beta_0, \frac{z_0}{H}\right) \qquad (27)$$

where $\bar{F}(\alpha, \beta_0, z_0/H)$ is given in Appendix A. The background and resonant responses are given in Eqs. (15) and (16).

Detailed expressions for the top displacement, bending moment and shear force at a given elevation z_0 are presented in closed-form in Appendix B. An alternative closed-form solution of the same wind load effects has been presented in Piccardo and Solari (2002) using a different approach. The background and resonant GRFs (BGRF and RGRF) for any response component
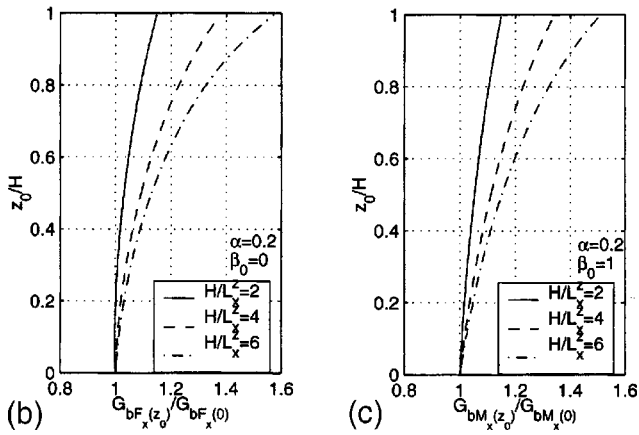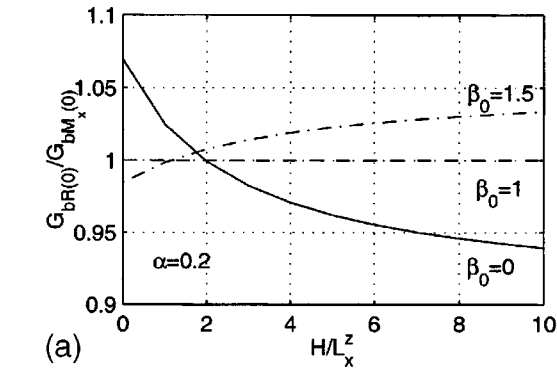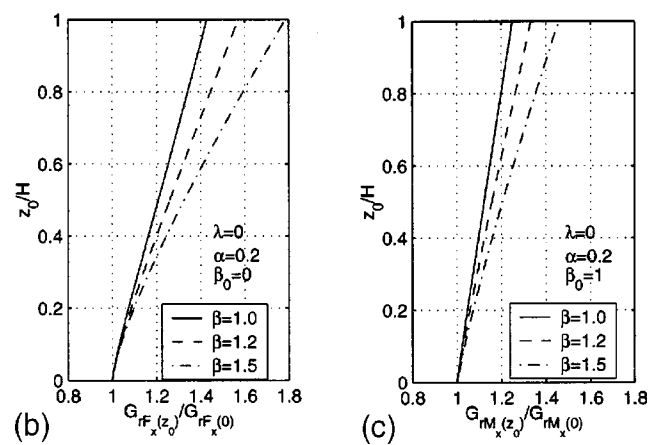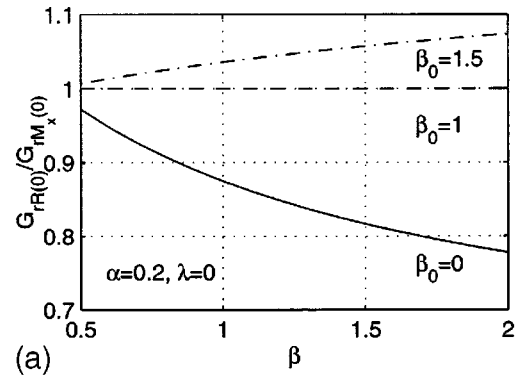
Fig. 3. Comparison of the background gust response factors: (a) base shear force, base bending moment and top displacement; (b) shear forces at different elevations; and (c) bending moments at different elevations
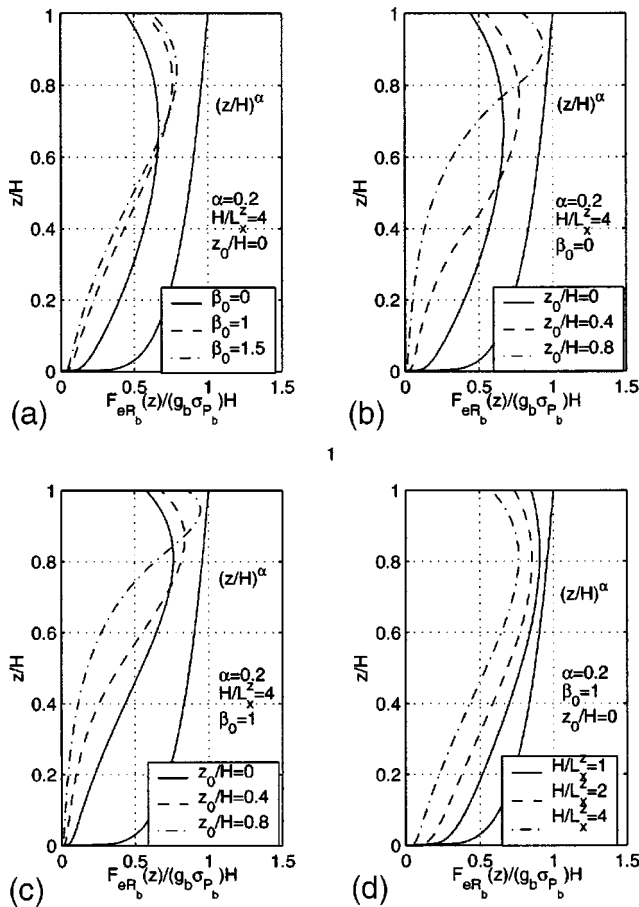

Fig. 4. Comparison of the resonant gust response factors: (a) base shear force, base bending moment and top displacement; (b) shear forces at different elevations; and (c) bending moments at different elevations

at any building elevation can be calculated as the ratio of the peak background and resonant components with respect to its mean value. For example, the BGRF and RGRF for the top displacement ($z_0 = 0$ and $\beta_0 = \beta'$), base bending moment ($z_0 = 0$ and $\beta_0 = 1$) and base shear force ($z_0 = 0$ and $\beta_0 = 0$) are given by the following general expressions:

$$G_b = \frac{g_b \sigma_{R_b}}{\bar{R}} = \frac{(1 + 2\alpha + \beta_0)}{(1 + \alpha + \beta_0)} \frac{2g_b I_u}{\sqrt{1 + H/L_u^z/(2.5 + \beta_0)}}$$

$$\times \sqrt{\int_0^{f_1} S_u^*(f)|\chi_D(f)|^2|J_y(f)|^2 df} \qquad (28)$$

$$G_r = \frac{g_r \sigma_{R_r}}{\bar{R}} = \frac{[(\beta + \beta_0 + 2) - \lambda(\beta + \beta_0 + 1)]}{(\beta + \beta_0 + 2)(\beta + \beta_0 + 1)}$$

$$\times \frac{(2\beta + 2)(2\beta + 1)}{[(2\beta + 2) - \lambda(2\beta + 1)]} \frac{(1 + 2\alpha + \beta_0)}{(1 + \alpha + \beta)}$$

$$\times \frac{2g_r I_u}{\sqrt{1 + k_z f_1 H/U_H/(2.5 + \beta)}}$$

$$\times \sqrt{\frac{\pi}{4\xi_1} f_1 S_u^*(f_1)|\chi_D(f_1)|^2|J_y(f_1)|^2} \qquad (29)$$

In order to highlight the dependence of GRF on the response under consideration, Fig. 3(a) shows the ratio of BGRFs for top displacement ($\beta' = \beta_0 = 1.5$ as an example) and base shear to the

BGRF for base bending moment. Figs. 3(b and c) compare BGRFs for shear and bending moment at different elevations, respectively, normalized by the BGRF for base shear and base bending moment, respectively. Fig. 4 shows the corresponding comparison results for the RGRFs.

It is noted that the differences among the BGRFs for base bending moment, base shear, and top displacement are marginal and are within 5%. Their influence on total peak responses will become less significant when the resonant components are included. However, the BGRFs for shear force and bending moment increase markedly with increasing elevation. This is due to the rapidly increasing value of the equivalent loads for responses at higher elevations as compared to the mean load. It is obvious that using the BGRF-based equivalent loading associated with either base bending moment, base shear or top displacement, that follows a distribution similar to the mean wind load, will remarkably underestimate the background responses at higher elevations.

On the other hand, as indicated in Fig. 4(a), the RGRF for the base shear force is remarkably different from those for the base bending moment and the top displacement. As shown in Figs. 4(b and c), the variations in RGRFs with elevation may be significant. This is due to the fact that the actual equivalent load distribution in terms of the inertial load may significantly deviate from the mean load distribution. Again, using the RGRF based equivalent load associated with the base bending moment or base shear or top displacement will introduce noteworthy errors in predicting other resonant responses at different elevations. The dependence
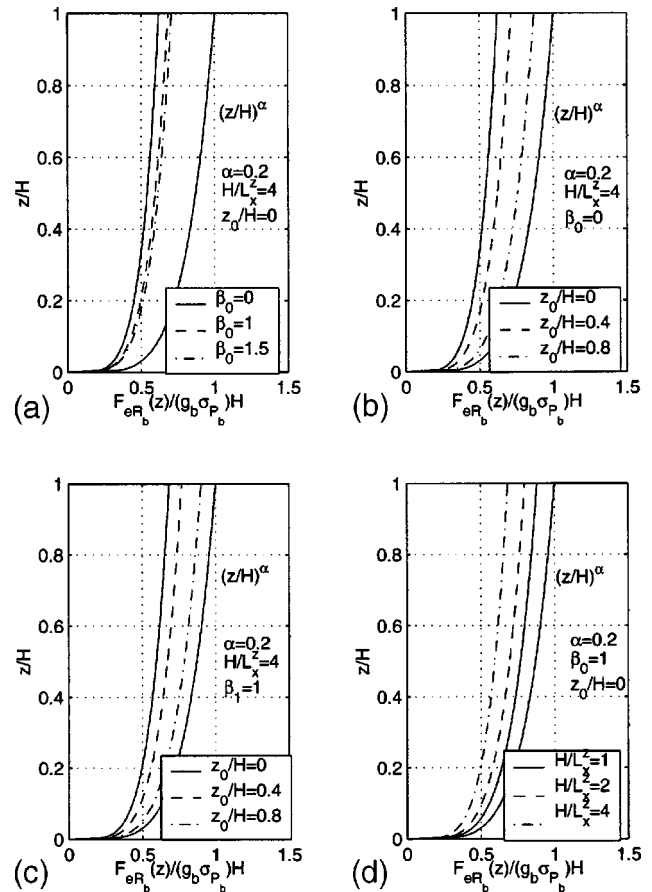
Fig. 5. Background equivalent static wind load distributions based on the load-response-correlation approach: (a) base shear force and bending moment and top displacement; (b) shear forces at different elevations; (c) bending moments at different elevations; and (d) base bending moment with different turbulence scales

Fig. 6. Background equivalent static wind load distributions based on the gust loading envelope approach: (a) base shear force, bending moment, and top displacement; (b) shear forces at different elevations; (c) bending moments at different elevations; and (d) base bending moment with different turbulence scales

of GRF on the response has also been discussed in Solari and Repetto (2002) based on a different approach.

Fig. 5 presents BESWLs based on the LRC approach. Fig. 5(a) provides BESWLs for base shear force ($z_0=0$ and $\beta_0=0$), base bending moment ($z_0=0$ and $\beta_0=1$) and top displacement ($z_0=0$ and β' is chosen as $\beta'=\beta_0=1.5$ as an example). Figs. 5(b and c) show those for shear force and bending moment at different elevations. The gust loading envelope is also shown that describes the envelope of the BESWL distribution. The differences in the background loads correspond to the reduction effects for different response components resulting from the loss of correlation in wind loads over the building height. As indicated by the load distributions for shear force and bending moment at $z_0=0.8H$ with $z \geq z_0$ in Figs. 5(b and c), the background loads associated with highly correlated localized wind load effects are close to the gust loading envelope. As suggested in Fig. 5(d), with an increase in wind load correlation that corresponds to the decrease in parameter H/L_x^z, the BESWLs based on the LRC approach are close to the gust loading envelope.

As expected, while LRC approach based BESWLs provide a physically meaningful load distribution, the dependence of their spatial distribution on the response being considered may preclude this load description for possible adoption by a building code or standard. On the other hand, the load distributions based on the GLE approach proposed in this study are similar to the

gust loading envelope for all response components which are scaled by the background factor as indicated by Fig. 6. This is similar to the traditional GRF approach, but the load distribution depends on the external fluctuating load rather than the mean load. In addition, the background factor, B_z, has a clearer physical meaning than the BGRF, G_b.

The advantage of expressing the RESWL in terms of the inertial loading is that it obviously leads to a single load distribution for all responses. However, significantly different GRFs and RESWLs are required for different response components when the traditional GRF approach is utilized with a load distribution similar to the mean load. The ESWL for total peak response based on external wind loads and modal inertial loads is particularly suited for the acrosswind and torsional responses in which the mean wind loads and responses are generally small which renders the ESWL based on the traditional GRF approach less appropriate for practical applications.

Equivalent Static Wind Loads Based on the High-Frequency Force Balance Technique

The HFFB technique has been widely utilized for estimating the generalized modal forces on buildings with uncoupled mode shapes. In this technique, base forces are measured on geometri-

cally scaled, light-weight, stiff building models (e.g., Kareem and Cermark 1979; Tschanz and Davenport 1983; Reinhold and Kareem 1986; Boggs and Peterka 1989). The estimated generalized modal force is then utilized to obtain dynamic response for a wide range of structural characteristics. In the following, the evaluation of the ESWL based on HFFB measurements is discussed in light of mode shape correction and the inherent uncertainty associated with the lack of information concerning spatiotemporal distribution of wind loads on the building surface.

For buildings with translational mode shapes varying nonlinearly over the building height, mode shape corrections are needed in estimating the generalized modal forces using the measured base bending moments. Considering wind loads and response in the translational direction, x, the mode shape correction factor for the generalized modal force is defined as

$$\eta_{Q_x} = \sqrt{\frac{S_{Q_x}(f_1)}{S_{M_x}(f_1)/H^2}} \tag{30}$$

which depends on the statistical features of the wind load, where S_{M_x}=PSD of the base bending moment on the stiff building model.

Accordingly, the resonant response given in Eq. (3) can be rewritten as

$$\sigma_{R_r} = \eta_{Q_x} \frac{\int_0^H m(z)\Theta_x(z)\mu_x(z)dz}{H\int_0^H m(z)\Theta_x^2(z)dz} \sqrt{\frac{\pi}{4\xi_1}f_1 S_{M_x}(f_1)} \tag{31}$$

Obviously, only the mode shape correction factor for the generalized modal force is needed when the actual building dynamic features are used in the response analysis.

However, when the actual building response with a nonlinear mode shape is directly evaluated from a "stick" aeroelastic building model with a linear mode shape, mode shape correction factors for each individual response are required (Zhou and Kareem 2003). Based on Eq. (31), the response of a building with a nonlinear mode shape, σ_{R_r}, can be expressed in terms of the response of a virtual building, $\sigma_{R_r}^0$, with identical geometrical features with the exception of a linear mode shape experiencing the same wind conditions, and a correction factor, η_R,

$$\sigma_{R_r} = \eta_R \sigma_{R_r}^0; \quad \eta_R = \eta_{0R}\eta_Q \tag{32}$$

$$\eta_{0R} = \frac{\int_0^H m(z)\Theta_x(z)\mu_x(z)dz}{\int_0^H m(z)\left(\frac{z}{H}\right)\mu_x(z)dz} \frac{\int_0^H m(z)\left(\frac{z}{H}\right)^2 dz}{\int_0^H m(z)\Theta_x^2(z)dz} \tag{33}$$

$$\sigma_{R_r}^0 = \frac{\int_0^H m(z)\left(\frac{z}{H}\right)\mu_x(z)dz}{\int_0^H m(z)\left(\frac{z}{H}\right)zdz} \sqrt{\frac{\pi}{4\xi_1}f_1 S_{M_x}(f_1)} \tag{34}$$

where η_{0R}=correction factor which depends only on building dynamics and can be evaluated accurately for a given building.

A host of studies concerning the mode shape correction factor based on wind tunnel studies or analytical models have been reported in Vickery et al. (1985), Boggs and Peterka (1989), Xu and
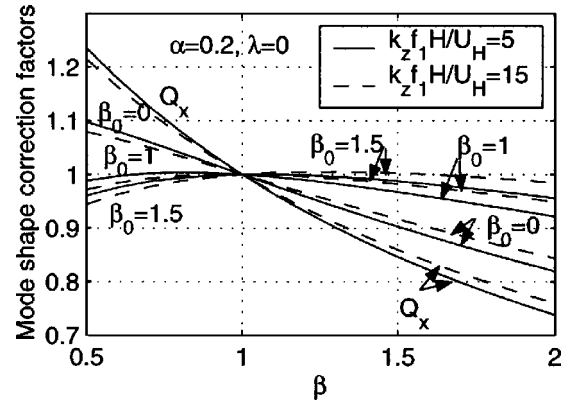
Fig. 7. Mode shape correction factors

Kwok (1993), and Zhou et al. (2002), among others. Formulations based on analytical models in the literature are often restricted to two limiting cases of the correlation level of wind loading along the building height, i.e., fully coherent and zero coherent. Using the analytical model presented in this study with the closed-form expression for joint acceptance, the influence of wind load coherence can be explicitly described by the parameter $k_z f_1 H/U_H$. Thus, the mode shape correction can be better quantified. For example, η_{Q_x} can be expressed as

$$\eta_{Q_x} = \frac{(2+\alpha)}{(1+\alpha+\beta)}\sqrt{\frac{1+k_z f_1 H/U_H/3.5}{1+k_z f_1 H/U_H/(2.5+\beta)}} \tag{35}$$

and η_{0R} is given in terms of the building dynamics as

$$\eta_{0R} = \frac{[(\beta+\beta_0+2)-\lambda(\beta+\beta_0+1)]}{(\beta+\beta_0+1)(\beta+\beta_0+2)} \frac{(\beta_0+2)(\beta_0+3)}{[(\beta_0+3)-\lambda(\beta_0+2)]}$$
$$\times \frac{(4-3\lambda)}{12} \frac{(2\beta+1)(2\beta+2)}{[(2\beta+2)-\lambda(2\beta+1)]} \tag{36}$$

where $\beta_0=\beta'$, 1, 0 for top displacement, base bending moment and base shear force, respectively. A similar expression for the mode shape correction factor for the generalized modal force was given in Marukawa et al. (1990).

Fig. 7 shows mode shape correction factors for the generalized modal force, top displacement, base bending moment, and base shear force. It is noted that mode shape correction factors for different responses have different magnitudes, but each has the same level of uncertainty as that implied in the correction factor for the generalized modal force, η_{Q_x}. Since only the measured base bending moment does not provide sufficient information concerning the spatiotemporal variations of wind loads on the building surface, the mode shape correction procedure has to rely on an empirical formulation or on a presumed analytical wind loading model. Therefore, this procedure introduces uncertainty in the predicted wind loads and the attendant responses due to the potential of inappropriate modeling of the actual wind loads. An accurate estimation of the mode shape correction factor becomes a more challenging task for buildings with complex geometries and 3D coupled mode shapes as well as for cases in which the mean wind directions are not normal to a building face.

By distributing the peak base bending moment response along the building height following the inertial load distribution the RESWL can be expressed as

$$F_{erx}(z) = \frac{g_r m(z)\Theta_x(z)}{\displaystyle\int_0^H m(z)\Theta_x(z)z\,dz}\sigma_{M_{xr}(0)} \qquad (37)$$

where $\sigma_{M_{xr}(0)}$ is given in Eqs. (32)–(34) with $R_r = M_{xr}(0)$ and $\mu_x(z) = z$.

Accordingly, the peak response of any given resonant response $R(z_0, t)$ can be calculated by a static analysis using the RESWL. Obviously, the correction factors for these responses actually need not be explicitly addressed while utilizing the RESWL, which is already incorporated through the corrected base bending moment and the associated RESWL.

A similar expression of the RESWL in terms of the base shear force distributed along the building height is widely utilized for describing the equivalent static earthquake load in building codes [e.g.,ASCE 7-02 (2002)]. However, the format based on the base bending moment response is becoming increasingly popular in describing wind loads on buildings (e.g., Zhou and Kareem 2001). As demonstrated in previous studies and is reconfirmed in Fig. 7, the mode shape correction factor for the base bending moment, η_{M_x}, is rather insensitive to the mode shape parameter β and is very close to unity (e.g., Zhou et al. 2002). While the empirical formulation of η_{M_x} is provided in some building codes and standards, in practice, η_{M_x} may even be approximated as unity for the simplicity necessary for design standards. However, it is worth mentioning that the base bending moment-based RESWL itself does not provide a superior estimate of the equivalent loading or response as compared to the RESWL based on base shear or other responses. This approach exhibits the same level of uncertainty as that implied in the estimate of the generalized modal force which manifests from the lack of information concerning spatiotemporal distribution of wind loading available from measured base bending moments.

Following the general expression for the background response in terms of the influence function [Eq. (2)], the background response is actually not influenced by the mode shape rather it depends on the influence function. As the background response is not amplified by building dynamics, the background shear force and bending moment can be directly measured through force balances using a stationary aerodynamic building model or using a stick aeroelastic building model. However, other response components such as displacement have to be estimated based on measured base forces with appropriate correction factors. Assuming that the analytical loading model presented in this study is valid, the RMS background response of $R(z_0, t)$ can be expressed in terms of the base bending moment as

$$\sigma_{R_b} = \frac{\mu_0 F_b\left(\alpha, \beta_0, \dfrac{z_0}{H}\right) B_z\left(\alpha, \beta_0, \dfrac{z_0}{H}\right)}{H F_b(\alpha, 1, 0) B_z(\alpha, 1, 0)}\sigma_{M_{xb}(0)} \qquad (38)$$

For example, following Eq. (38), the RMS background top displacement is given by

$$\sigma_{Y_{xb}} = \frac{i_0}{H}\frac{(2+\alpha)}{(1+\alpha+\beta')}\sqrt{\frac{1+H/L_x^z/3.5}{1+H/L_x^z/(2.5+\beta')}}\,\sigma_{M_{xb}(0)} \qquad (39)$$

and the expression for the base shear can be given by setting $i_0 = 1$ and $\beta' = 0$ in the preceding formulation, where $\sigma_{M_{xb}(0)} =$ RMS background base bending moment.

Comparing Eq. (39) to Eq. (35), it is obvious that the influence of coefficients α, β', and H/L_x^z on the background response is

similar to the coefficients α, β, and $k_z f_1 H/U_H$ involved in the mode shape correction factor for the generalized modal force.

It is noted that when both the base bending moment, $M_x(t)$, and base shear force, $F_x(t)$, are measured using a stationary building model, and the analytical loading model is applicable, the parameters of k_z, L_x^z, and $S_P(f)$ can be identified by fitting the measured data. Subsequently, the distribution of external wind loads can be quantified completely, and any response and associated ESWL including the background and resonant components can be determined based on the model.

Unless an analytical model is applicable or certain assumptions are made, predictions of the background response and BESWL remain a challenging task with the information restricted to the measured base bending moments. Correlation factors for background responses have been addressed in literature using an analytical model for the two limiting cases with an implicit assumption that neglects the contribution of higher modes (Boggs and Peterka 1989; Zhou et al. 2002). As discussed earlier, by neglecting higher-mode contributions to the background response, the background response analysis, mode shape correction and BESWL can be estimated readily using the formulations akin to the resonant components utilizing base bending moment measurement. Assuming that the BESWL is similar to the mean wind load distribution, the background response can also be estimated from the measurement of base bending moment.

To address the contributions of higher building modes to the background response, the ratio of the response based on the fundamental modal response with respect to one obtained by employing the influence function is calculated following the analytical model:

$$\frac{\sigma'_{R_b}}{\sigma_{R_b}} = F_r\left(\beta, \beta_0, \frac{z_0}{H}\right)\frac{F_b(\alpha, \beta, 0)}{F_b\left(\alpha, \beta_0, \dfrac{z_0}{H}\right)}\frac{B_z(\alpha, \beta, 0)}{B_z\left(\alpha, \beta_0, \dfrac{z_0}{H}\right)} \qquad (40)$$

When $z_0 = 0$, it reduces to

$$\begin{aligned}
\frac{\sigma'_{R_b}}{\sigma_{R_b}} = {} & \frac{[(\beta+\beta_0+2)-\lambda(\beta+\beta_0+1)]}{(\beta+\beta_0+1)(\beta+\beta_0+2)}\frac{(2\beta+1)(2\beta+2)}{[(2\beta+2)-\lambda(2\beta+1)]}\\
& \times\frac{(1+\alpha+\beta_0)}{(1+\alpha+\beta)}\sqrt{\frac{1+H/L_x^z/(2.5+\beta_0)}{1+H/L_x^z/(2.5+\beta)}}
\end{aligned} \qquad (41)$$

where $\beta_0 = \beta'$, 1 and 0 represent for the top displacement, base bending moment, and base shear force, respectively. It is noted that $\beta = \beta_0$ leads to $\sigma'_{R_b}/\sigma_{R_b} = 1$, indicating that for buildings with linear mode shapes, the base bending moment calculated in the fundamental modal response is actually the same as that from the influence function. The same conclusion applies to the top displacement when its influence function is approximated as proportional to the fundamental mode shape.

Fig. 8 suggests that the fundamental modal response provides a good approximation of the base bending moment and top displacement, but remarkably underestimates the base shear force. The higher-mode contributions become more significant for background response in the cases of relatively stiffer buildings.

Concluding Remarks

A framework for evaluating the equivalent static wind load for any peak response component of buildings with uncoupled responses in three primary directions was presented. The equivalent
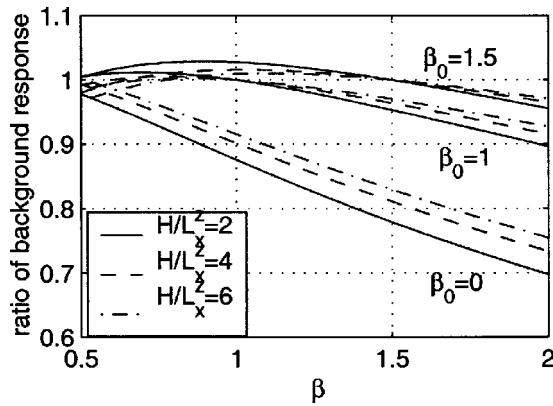
Fig. 8. Contributions of higher modes to the background responses

static wind load was expressed as a linear combination of the background and resonant loads. The background and resonant components of loading were derived using the concept of gust loading envelope and the distribution of inertial loads in the fundamental structural modes in each direction. The proposed background load based on the GLE offered a very simplified load description in comparison with the load-response-correlation approach whose spatial distribution exhibits dependence on the response component of interest. It also provided a physically more-meaningful and efficacious description of the loading as compared to the gust response factor approach.

Closed-form formulations were presented based on an analytical wind loading model. The gust response factors for various alongwind response components at various building elevations were presented in closed-form and compared to highlight the variations inthe gust response factors for different response components. It was pointed out that using the equivalent static wind load associated with base bending moment, base shear, or top displacement that followed a distribution similar to the mean wind load may introduce noteworthy errors in the estimation of other responses at all elevations. The proposed equivalent static wind load in terms of the external fluctuating wind load and inertial load provided a convenient and meaningful load description for potential applications to building codes and standards.

Formulations for mode shape correction factors needed in the HFFB technique or stick aeroelastic building model tests were presented based on an analytical loading model. These formulations offered a clear relationship to the spatial coherence characteristics of wind loads and promised to provide a more accurate estimate when compared to the formulations given in literature which relied on the two limiting cases of the correlation levels of wind loading. It was emphasized that mode shape correction factors for different response components have varying magnitudes but exhibit the same level of uncertainty as implied in the estimation of the generalized modal force. This was attributed to the lack of information concerning the spatiotemporal distribution of wind loading knowing only the measured base bending moment. When the concept of equivalent static wind loading in terms of the base bending moment distributed over the building height was employed, following the inertial load distribution, only the mode shape correction for the base bending moment explicitly appeared in the estimated response. This format is becoming increasingly popular in describing wind loads on buildings. However, it was pointed out that this format does not provide a superior estimate of the equivalent loading or response as compared to the procedure based on the base shear or other responses regarding the uncertainty of estimation when only limited loading information is available. The approximation of background response by the fundamental modal response often used in literature may significantly underestimate the base shear response.

Acknowledgment

Appendix I. Functions Used in the Background and Resonant Responses

$$\bar{F}\left(\alpha, \beta_0, \frac{z_0}{H}\right) = \frac{1}{H}\int_{z_0}^{H}\left(\frac{z-z_0}{H}\right)^{\beta_0}\left(\frac{z}{H}\right)^{2\alpha}dz \tag{42}$$

$$F_b\left(\alpha, \beta_0, \frac{z_0}{H}\right) = \frac{1}{H}\int_{z_0}^{H}\left(\frac{z_1-z_0}{H}\right)^{\beta_0}\left(\frac{z_1}{H}\right)^{\alpha}dz_1 \tag{43}$$

$$F_r\left(\beta, \beta_0, \frac{z_0}{H}\right) = \left(\int_{z_0}^{H}m(z)\left(\frac{z}{H}\right)^{\beta}\left(\frac{z-z_0}{H}\right)^{\beta_0}dz\right)\Bigg/\left(\int_{0}^{H}m(z)\left(\frac{z}{H}\right)^{2\beta}dz\right) \tag{44}$$

$$B_z^2\left(\alpha, \beta_0, \frac{z_0}{H}\right) = \frac{\int_{z_0}^{H}\int_{z_0}^{H}\left(\frac{z_1-z_0}{H}\right)^{\beta_0}\left(\frac{z_2-z_0}{H}\right)^{\beta_0}\left(\frac{z_1}{H}\right)^{\alpha}\left(\frac{z_2}{H}\right)^{\alpha}\exp\left(-\frac{|z_1-z_2|}{L_x^z}\right)dz_1 dz_2}{\int_{z_0}^{H}\int_{z_0}^{H}\left(\frac{z_1-z_0}{H}\right)^{\beta_0}\left(\frac{z_2-z_0}{H}\right)^{\beta_0}\left(\frac{z_1}{H}\right)^{\alpha}\left(\frac{z_2}{H}\right)^{\alpha}dz_1 dz_2} \tag{45}$$

$$|J_z(\alpha,\beta,f)|^2 = \frac{(1+\alpha+\beta)^2}{H^2} \int_0^H \int_0^H \left(\frac{z_1}{H}\right)^{\alpha+\beta} \left(\frac{z_2}{H}\right)^{\alpha+\beta} \exp\left(-\frac{k_zf|z_1-z_2|}{U_H}\right) dz_1 dz_2 \tag{46}$$

Appendix II. Displacement, Bending, and Shear Force Responses

Based on the analytical model for the fluctuating wind load, the background and resonant components of the top displacement $Y_x(t)$, bending moment, and shear force at a building elevation z_0 above the ground, $M_x(z_0,t)$ and $F_x(z_0,t)$, can be expressed as follows:

$$\sigma_{Y_{xb}} = i_0 F_b(\alpha,\beta',0) B_z(\alpha,\beta',0)\sigma_{P_b} \tag{47}$$

$$\sigma_{M_{xb}}(z_0) = HF_b\left(\alpha,1,\frac{z_0}{H}\right) B_z\left(\alpha,1,\frac{z_0}{H}\right)\sigma_{P_b} \tag{48}$$

$$\sigma_{F_{xb}}(z_0) = F_b(\alpha,0,z_0/H) B_z\left(\alpha,0,\frac{z_0}{H}\right)\sigma_{P_b} \tag{49}$$

$$\sigma_{Y_{xr}} = i_0 F_r(\beta,\beta',0)\frac{|J_z(\alpha,\beta,f_1)|}{(1+\alpha+\beta)}\sqrt{\frac{\pi}{4\xi_1}f_1 S_P(f_1)} \tag{50}$$

$$\sigma_{M_{xr}}(z_0) = HF_r\left(\beta,1,\frac{z_0}{H}\right)\frac{|J_z(\alpha,\beta,f_1)|}{(1+\alpha+\beta)}\sqrt{\frac{\pi}{4\xi_1}f_1 S_P(f_1)} \tag{51}$$

$$\sigma_{F_{xr}}(z_0) = F_r\left(\beta,0,\frac{z_0}{H}\right)\frac{|J_z(\alpha,\beta,f_1)|}{(1+\alpha+\beta)}\sqrt{\frac{\pi}{4\xi_1}f_1 S_P(f_1)} \tag{52}$$

where

$$F_b(\alpha,\beta',0) = \frac{1}{(1+\alpha+\beta')} \tag{53}$$

$$F_b\left(\alpha,1,\frac{z_0}{H}\right) = \left[\frac{1}{\alpha+2} - \frac{1}{\alpha+1}\left(\frac{z_0}{H}\right)\right.$$
$$\left. + \frac{1}{(\alpha+2)(\alpha+1)}\left(\frac{z_0}{H}\right)^{\alpha+2}\right] \tag{54}$$

$$F_b\left(\alpha,0,\frac{z_0}{H}\right) = \frac{1}{(\alpha+1)}\left[1-\left(\frac{z_0}{H}\right)^{\alpha+1}\right] \tag{55}$$

$$B_z\left(\alpha,\beta_0,\frac{z_0}{H}\right) \approx \frac{1}{\sqrt{1+(H-z_0)/L_{u'}^z/(2.5+\beta_0)}}$$
$$(\beta_0 = \beta',1,0) \tag{56}$$

$$F_r(\beta,\beta',0) = \frac{[(\beta+\beta'+2)-\lambda(\beta+\beta'+1)]}{(\beta+\beta'+1)(\beta+\beta'+2)}$$
$$\times\frac{(2\beta+1)(2\beta+2)}{[(2\beta+2)-\lambda(2\beta+1)]} \tag{57}$$

$$F_r\left(\beta,1,\frac{z_0}{H}\right) = \left[\frac{(\beta+1)-(\beta+2)\left(\frac{z_0}{H}\right)+\left(\frac{z_0}{H}\right)^{\beta+2}}{(\beta+1)(\beta+2)}\right.$$
$$\left. -\lambda\frac{(\beta+2)-(\beta+3)\left(\frac{z_0}{H}\right)+\left(\frac{z_0}{H}\right)^{\beta+3}}{(\beta+2)(\beta+3)}\right]$$
$$\times\frac{(2\beta+1)(2\beta+2)}{[(2\beta+2)-\lambda(2\beta+1)]} \tag{58}$$

$$F_r\left(\beta,0,\frac{z_0}{H}\right) = \left[\frac{1-\left(\frac{z_0}{H}\right)^{\beta+1}}{\beta+1} - \lambda\frac{1-\left(\frac{z_0}{H}\right)^{\beta+2}}{\beta+2}\right]$$
$$\times\frac{(2\beta+1)(2\beta+2)}{[(2\beta+2)-\lambda(2\beta+1)]} \tag{59}$$

$$|J_z(\alpha,\beta,f_1)| \approx \frac{1}{\sqrt{1+k_zf_1H/U_H/(2.5+\beta)}} \tag{60}$$

$$i_0 = \frac{1}{m_0 H(2\pi f_1)^2}\frac{(\beta+\beta'+1)(\beta+\beta'+2)}{[(\beta+\beta'+2)-\lambda(\beta+\beta'+1)]} \tag{61}$$

When the wind direction aligns with the translational axis x, the mean response in the same direction (alongwind response) is expressed as

$$\bar{Y}_x = q_H i_0 \bar{F}(\alpha,\beta',0) = \frac{q_H i_0}{2\alpha+\beta'+1} \tag{62}$$

$$\bar{M}_x(z_0) = q_H H\bar{F}\left(\alpha,1,\frac{z_0}{H}\right) = q_H H\left[\frac{1}{2\alpha+2} - \frac{1}{2\alpha+1}\left(\frac{z_0}{H}\right)\right.$$
$$\left. + \frac{1}{(2\alpha+1)(2\alpha+2)}\left(\frac{z_0}{H}\right)^{2\alpha+2}\right] \tag{63}$$

$$\bar{F}_x(z_0) = q_H\bar{F}\left(\alpha,0,\frac{z_0}{H}\right) = \frac{q_H}{2\alpha+1}\left[1-\left(\frac{z_0}{H}\right)^{2\alpha+1}\right] \tag{64}$$

References

American Society of Civil Engineers (ASCE). (2002). "Minimum design loads for buildings and other structures." *ASCE 7-02*, New York.

Boggs, D. W., and Peterka, J. A. (1989). "Aerodynamic model tests of tall buildings." *J. Eng. Mech.*, 115(3), 618–635.

Chen, X., and Kareem, A. (2000). "On the application of stochastic decomposition in the analysis of wind effects." *Advances in structural dynamics, ASD 2000*, J. M. Ko and Y. L. Xu, eds., Elsevier, Amsterdam, The Netherlands, *Proc., Int. Conf. on Advances in Structural Dynnamics (ASD 2000)*, Hong Kong, China, 135–142.

Chen, X., and Kareem, A. (2001). "Equivalent static wind loads for buf-

feting response of bridges." *J. Struct. Eng.*, 127(12), 1467–1475.

Davenport, A. G. (1967). "Gust loading factors." *J. Struct. Div. ASCE*, 93(1), 11–34.

Davenport, A. G. (1985). "The representation of the dynamic effects of turbulent wind by equivalent static wind loads." *AISC/CISC Int. Symp. Structural Steel*, Chicago, 3-1-3-13.

European Committee for Standardization (CEN). (1994) "Eurocode 1: Basis of design and actions on structures. Part 2-4:Wind actions." *ENV-1991-2-4*, CEN, Brussels.

Holmes, J. D. (1994). "Along-wind response of lattice towers. I: Derivation of expression for gust response factors." *Eng. Struct.*, 16, 287–292.

Holmes, J. D. (1996). "Along-wind of lattice towers. III: Effective load distribution." *Eng. Struct.*, 18, 483–488.

Holmes, J. D. (2002a). "Gust loading factor to dynamic response factor (1967-2002)." Symp. Preprints, Engineering, Symp. to Honor Alan G. Davenport for his 40 years of Contributions, The Univ. of Western Ontario, London, Ont., Canada, June 20-22, A1–1–A1–8,

Holmes, J. D. (2002b). "Effective static load distributions in wind engineering." *J. Wind. Eng. Ind. Aerodyn.*, 90, 91–109

Holmes, J. D., and Kasperski, M. (1996). "Effective distributions of fluctuating and dynamic wind loads." *Australian Civil/Struct. Eng. Trans.*, 38, 83–88.

Isyumov, N. (1999). "Overview of wind action on tall buildings and structures." *Wind Engineering into 21st Century*, Larsen, Larose, and Livesey, eds., Balkema, Rotterdam, The Netherlands, Proc., 10th Int. Conf. on Wind Eng., Copenhagen, Denmark, 15–18.

Kareem, A., and Cermark, J. E. (1979). "Wind tunnel simulation of wind-structure interactions." *ISA Trans.*, 18(4), 23–41.

Kareem, A., and Chen, X. (2004). "Wind effects on tall buildings in Urban Environment." *Proc., 1st Int. Conf on Wind Effects on Buildings and Urban Environment*, Wind Engineering Research Center, Tokyo Polytechnic Univ., Japan.

Kareem, A., and Zhou, Y. (2003). "Gust loading factor—Past, present, and future." *J. Wind. Eng. Ind. Aerodyn.*, 91(12–15), 1301–1328.

Kasperski, M. (1992). "Extreme wind load distributions for linear and nonlinear design." *Eng. Struct.*, 14, 27–34.

Marukawa, H., Ohkuma, T., and Momomura, Y. (1990). "Estimation of across-wind and torsional acceleration of prismatic high rise buildings." *Proc., 11th Natl. Symp. on Wind Engineering*, Japan Association for Wind Engineering, Tokyo, Japan, 215–220.

Piccardo, G., and Solari, G. (2000). "Three-dimensional wind-excited response of slender structures: Closed-form solution." *J. Struct. Eng.*, 126(8), 936–943.

Piccardo, G., and Solari, G. (2002). "3D gust effect factor for slender vertical structures." *Probab. Eng. Mech.*, 17, 143–155.

Reinhold, T. A., and Kareem, A. (1986). "Wind loads and building response predictions using force balance techniques." *Proc., 3rd ASCE Engineering Mechanics Conf.-Dynamics of Structures*, Univ. of California, Los Angeles, 380–397.

Repetto, M. P., and Solari, G. (2004). "Equivalent static wind actions on vertical structures." *J. Wind. Eng. Ind. Aerodyn.*, 100(7), 1032–1040.

Solari, G., and Repetto, M. P. (2002). "General tendencies and classification of vertical structures under wind loads." *J. Wind. Eng. Ind. Aerodyn.*, 90, 1299–1319.

Tamura, Y., Kikuchi, H., and Hibi, K. (2002). "Actual extreme pressure distributions and LRC formula." *J. Wind. Eng. Ind. Aerodyn.*, 90, 1959–1971.

Tschanz, T., and Davenport, A. G. (1983). "The base balance technique for the determination of dynamic wind loads." *J. Wind. Eng. Ind. Aerodyn.*, 13(1–3), 429–439.

Vickery, P. J., Steckley, A. C., Isyumov, N., and Vickery, B. J. (1985). "The effect of mode shape on the wind induced response of tall buildings." *Proc., 5th U.S. Natl. Conf. on Wind Engineering*, American Association for Wind Engineering, Texas Tech Univ., Lubbock, Tex., 1B-41-1B-48.

Xu, Y. L., and Kwok, K. C. S. (1993). "Mode shape corrections for wind tunnel tests of tall buildings." *Eng. Struct.*, 15, 618–635.

Zhou, Y., Kareem, A., and Gu, M., (2000). "Equivalent static buffeting loads on structures." *J. Struct. Eng.*, 126(8), 989–992.

Zhou, Y., and Kareem, A. (2001). "Gust loading factor: New model." *J. Struct. Eng.*, 127(2), 168–175.

Zhou, Y., Kareem, A., and Gu, M. (2002). "Mode shape corrections for wind load effects." *J. Eng. Mech.*, 128(1), 15–23.

Zhou, Y., and Kareem, A. (2003). "Aeroelastic balance." *J. Eng. Mech.*, 129(3), 283–292.